

Symmetry breaking in merging binary black holes from young massive clusters and isolated binaries

SAMBARAN BANERJEE,^{1,2} ALEKSANDRA OLEJAK,³ AND KRZYSZTOF BELCZYNSKI³

¹ *Helmholtz-Institut für Strahlen- und Kernphysik, Nussallee 14-16, D-53115 Bonn, Germany*

² *Argelander-Institut für Astronomie, Auf dem Hügel 71, D-53121, Bonn, Germany*

³ *Nicolaus Copernicus Astronomical Center, Polish Academy of Sciences, Bartycka 18, 00-716 Warsaw, Poland*

ABSTRACT

Properties of the to-date-observed binary black hole (BBH) merger events suggest a preference towards spin-orbit aligned mergers. Naturally, this has caused widespread interest and speculations regarding implications on various merger formation channels. Here we show that (i) not only the BBH-merger population from isolated binaries but also (ii) BBH population formed in young massive clusters (YMC) would possess an asymmetry in favour of aligned mergers, in the distribution of the events' effective spin parameter (χ_{eff}). In our analysis, we utilize BBH-merger outcomes from state-of-the-art N-body evolutionary models of YMCs and isolated binary population synthesis. We incorporate, for the first time in such an analysis, misalignments due to both natal kicks and dynamical encounters. The YMC χ_{eff} distribution has a mean (an anti-aligned merger fraction) of $\langle \chi_{\text{eff}} \rangle \leq 0.04$ ($f_X - \approx 40\%$), which is smaller (larger) than but consistent with the observed asymmetry of $\langle \chi_{\text{eff}} \rangle \approx 0.06$ ($f_X - \approx 28\%$) as obtained from the population analysis by the LIGO-Virgo-KAGRA collaboration. In contrast, isolated binaries alone tend to produce a much stronger asymmetry; for the tested physical models, $\langle \chi_{\text{eff}} \rangle \approx 0.25$ and $f_X - \lesssim 7\%$. Although the YMC χ_{eff} distribution is more similar to the observed counterpart, none of the channels correctly reproduce the observed distribution. Our results suggest that further extensive model explorations for both isolated-binary and dynamical channels as well as better observational constraints are necessary to understand the physics of 'the symmetry breaking' of the BBH-merger population.

Keywords: Stellar mass black holes (1611); Massive stars (732); N-body simulations (1083); Gravitational wave sources (677); Close binary stars (254); Young massive clusters (2049)

1. INTRODUCTION

We are on the verge of a 'golden era' of gravitational-wave (GW) and multi-messenger astronomy (Branchesi 2016; Mapelli 2018; Mészáros et al. 2019; Mandel & Broekgaarden 2022; Spera et al. 2022). Until now, the LIGO-Virgo-KAGRA collaboration (LVK; Aasi et al. 2015; Acernese et al. 2015; KAGRA Collaboration et al. 2020) has published, in their GW transient catalogue (GWTC) ¹, nearly 90 candidates of general relativis-

tic (GR) compact binary merger events. The current GWTC includes all event candidates from LVK's first, second ('O1', 'O2'; Abbott et al. 2019), and third ('O3'; Abbott et al. 2021a,b) observing runs, including those in their 'Deep Extended Catalogue' (Abbott et al. 2021c).

In this study, we focus on a specific feature of GWTC, namely, the apparent asymmetry around zero of the distribution of the effective spin parameters in the observable merging binary black hole (BBH) population. The effective spin parameter (Ajith et al. 2011), χ_{eff} , of a GR-merging binary is a measure of the spin-orbit alignment of the system and is defined as

$$\chi_{\text{eff}} \equiv \frac{M_1 |\vec{a}_1| \cos \theta_1 + M_2 |\vec{a}_2| \cos \theta_2}{M_1 + M_2} = \frac{|\vec{a}_1| \cos \theta_1 + q |\vec{a}_2| \cos \theta_2}{1 + q} \quad (1)$$

sambaran.banerjee@gmail.com

aleksandra.olejak@wp.pl

chrisbelczynski@gmail.com

¹ <https://www.gw-openscience.org/eventapi/html/GWTC/>

Here, the merging masses M_1 , M_2 , with mass ratio $q \equiv M_2/M_1$ ($q \leq 1$), have, respectively, Kerr vectors \vec{a}_1 , \vec{a}_2 that project with angles θ_1 , θ_2 on the orbital angular momentum vector just before the merger.

LVK’s recent population analyses suggest that merging BBHs of the Universe can be both aligned ($\chi_{\text{eff}} > 0$) or anti-aligned ($\chi_{\text{eff}} < 0$). However, aligned mergers are preferred over their anti-aligned counterparts. This is apparent from, *e.g.*, Figure 16 of Abbott et al. (2023). It is important to note that the observed GW events do *not* support a predominantly highly aligned or anti-aligned BBH merger population either; the χ_{eff} distribution in Abbott et al. (2023) is only slightly asymmetric around zero with a mean of $\langle \chi_{\text{eff}} \rangle = 0.06$, a standard deviation (SD) of $S_X = 0.10$, and a fraction of mergers with $\chi_{\text{eff}} < 0$ of 28% (see Table 1; below). Naturally, this peculiarity has sparked widespread interest in communities that study various mechanisms of forming merging compact binaries.

Notably, some previous analyses of GW population such as Galadage et al. (2021) and Roulet et al. (2021), covering events up to the LIGO–Virgo O3a observing run, find no evidence for negative- χ_{eff} systems, with the subpopulation of $\chi_{\text{eff}} < 0$ BBH mergers being model-dependent and coming from a population of mergers involving vanishing-spin BHs. They also find that a symmetric $\chi_{\text{eff}} < 0$ distribution is rather disfavored and that the concurrent event population can be reconstructed by isolated-binary evolution alone. However, the latest LVK population study (Abbott et al. 2023), that includes all O3 events, as well as a few other alternative analyses, *e.g.*, Callister et al. (2022); Callister & Farr (2023) infer that BH spin orientations span a wide range of spin-orbit misalignment angles, finding evidences for significantly misaligned and anti-aligned mergers. In particular, Callister et al. (2022) and Abbott et al. (2023) also apply an ‘extended’ BH-spin ansatz that explicitly includes a population of vanishing-spin BBH mergers, as in Galadage et al. (2021), but still infer a subpopulation of events with $\chi_{\text{eff}} < 0$. On the other hand, these studies also suggest that the χ_{eff} distribution is unlikely to be completely isotropic. The actual negative- χ_{eff} fraction is currently uncertain, and in this paper we adopt that from the most recent LVK population study (Abbott et al. 2023) (see below).

In dynamical BBH-merger formation in, *e.g.*, globular, open, and nuclear clusters, one generally expects a χ_{eff} distribution that is symmetric around zero, owing to the random and uncorrelated pairing of BHs (*e.g.*, Rodriguez et al. 2018; Arca Sedda et al. 2021). But Olejak & Belczynski (2021) have shown that such a ‘symmetry

breaking’² phenomenon is natural for merging BBHs formed out of isolated evolution of stellar binaries, once misalignment due to the BHs’ natal kicks is taken into account. An isolated binary evolution channel may be consistent with LVK χ_{eff} spin distribution while assuming effective angular momentum transport in massive stars combined with the possibility of Wolf-Rayet tidal spin-up (*e.g.* Olejak & Belczynski 2021; Fuller & Lu 2022; Carole et al. 2023). That allows to derive a distribution dominated by low BH spins, with an appropriate fraction of high-spinning BHs. Tauris (2022) has additionally considered the effect of BH spin-axis tossing in their isolated binary evolution model.

Trani et al. (2021), on the other hand, have demonstrated that an LVK-like symmetry breaking can as well occur solely due to misalignment introduced to BBHs (derived from interacting star-star binaries) via dynamical binary-single encounters inside young star clusters. Wang et al. (2021) have shown that symmetry breaking in dynamical interactions involving BBHs (and hence in their outcomes such as BBH mergers) is natural in coplanar dynamical systems, such as the gas disk of an active galactic nucleus (AGN), as opposed to dynamical pairing in (near) spherical stellar clusters.

In this work, we consider potential symmetry breaking in the BBH-merger population originating from young massive clusters (YMC) and from isolated binaries of the Universe. Binary evolution naturally leads to symmetry breaking, as majority of BBH mergers form from stars with mostly aligned spins due to binary interactions (leading to positive χ_{eff}), with some counteracting effect introduced by natal kicks that compact objects may receive (allowing for negative χ_{eff} ; *e.g.*, Gerosa & Berti 2017; Gerosa & Fishbach 2021). By virtue of the clusters’ young age ($\lesssim 100$ Myr), an observable BBH merger population, coming from YMCs, would comprise comparable proportions of primordially paired (*i.e.*, where the original binary membership is maintained; see Sec. 2.3) and dynamically assembled events (Belczynski et al. 2022a). The primordially paired mergers, due to their potential past binary-interaction phase, would introduce a non-randomness or symmetry breaking into the population. Here, we perform a preliminary study of the extent of this symmetry breaking, based on a set of realistic N-body-evolutionary models of YMCs. In our calculations, we explicitly incorporate spin-orbit misalignments due to remnant natal kick (based on a

² In this work, the term symmetry breaking refers to simply the deviation of the mean χ_{eff} from zero. More formal symmetry-related statistics such as skewness and moments of the χ_{eff} distribution will be considered in a follow up work.

binary population synthesis model) and dynamical encounters (based on numerical scattering experiments). That way, this study, for the first time, incorporates both the effects of natal kick and dynamical encounters in estimating the χ_{eff} distribution of a merging BBH population.

This paper is organized as follows. In Sec. 2.1 and 2.2 we summarize our isolated-binary and YMC models, respectively. We describe the models of BH spin and BBH-merger spin-orbit alignment in Sec. 2.3. Sec. 3 describes our results. In Sec. 4, we summarize our study and identify caveats and prospects for improvement.

2. METHODS

2.1. Evolutionary models of isolated-binary populations

We use a database of properties of isolated binary BBHs generated with **StarTrack** population synthesis code (Belczynski et al. 2020). The database has already been used and described in Olejak & Belczynski (2021). For the tested evolutionary model (hereafter CE21), we assume standard, non-conservative common envelope (CE) development criteria (Belczynski et al. 2008) for which the majority of BBHs form through CE evolution. For CE outcomes, we use the α_{CE} formalism (Webbink 1984) with orbital energy transfer for CE ejection $\alpha_{\text{CE}} = 1$ and binding parameter value λ based on Xu & Li (2010). We adopt a 5% Bondi accretion rate onto the BHs during CE (MacLeod et al. 2017). We adopt the delayed core-collapse supernova (SN) engine (Fryer et al. 2012) for the final compact object mass calculations and weak mass loss from pulsation pair-instability supernovae (Belczynski et al. 2016). For BH natal kick velocities, we adopt a Maxwellian distribution with one-dimensional dispersion $\sigma = 265 \text{ km s}^{-1}$ (Hobbs et al. 2005), which is lowered by fallback (Fryer et al. 2012) at the compact object formation. We adopt massive O/B star wind losses as in Vink et al. (2001), with additional LBV winds according to prescriptions listed in Sec. 2.2 of Belczynski et al. (2010). The population synthesis assumes the cosmic star formation rate and cosmic mean metallicity evolutions of Madau & Fragos (2017); for the metallicity evolution, a Gaussian spread of 0.5 dex ($Z_{\odot} = 0.014$) is assumed (Belczynski et al. 2020).

In Appendix A, we additionally provide results for a second model (hereafter RLOF21) which differs from CE21 only by the much more conservative criteria for CE development introduced in Olejak et al. (2021). The revised criteria (based on Pavlovskii et al. 2017), besides having more restricted conditions for the mass ratio, take into account metallicity and the donor’s radius to decide whether the system enters a CE phase. The

revised criteria result in a change of the dominant formation scenario for BBH mergers which, instead of CE, consists of two stable RLOF episodes.

2.2. Many-body evolutionary models of young massive clusters

In this study, the evolutionary models of YMCs, as described in Banerjee (2022a, hereafter Ba22), are utilized. All the details of these direct-N-body-computed model star clusters are elaborated in the Ba22 paper. Therefore, only a summary is provided below.

In Ba22, model star clusters of initial mass $M_{\text{cl}} = 7.5 \times 10^4 M_{\odot}$ (initial number of stars $N \approx 1.28 \times 10^5$) and initial size (half-mass radius) $r_{\text{h}} = 2 \text{ pc}$ were taken to be representatives of YMCs. Such cluster mass and size are comparable to those of most massive Galactic and local-group YMCs and moderate mass ‘super star clusters’ (Portegies Zwart et al. 2010; Krumholz et al. 2019). The initial density and kinematic profiles of the clusters followed the King (1966) model. A total of 40 models with King dimensionless potential $W_0 = 7$ and 9 and metallicities $Z = 0.0002, 0.001, 0.005, 0.01,$ and 0.02 (4 models generated with different random seeds for each W_0, Z combination) were evolved for 300 Myr (see Table A.1. of Ba22).

The initial cluster models comprised zero age main sequence (ZAMS) stars of masses $0.08 M_{\odot} \leq m_* \leq 150.0 M_{\odot}$ and distributed according to the canonical initial mass function (IMF; Kroupa 2001). The overall (initial) primordial-binary fraction was taken to be $f_{\text{bin}} = 5\%$. However, the initial binary fraction of O-type stars ($m_* \geq 16.0 M_{\odot}$), which were initially paired only among themselves, was $f_{\text{Obin}}(0) = 100\%$, consistently with the observed high binary fraction among O-stars in young clusters and associations (e.g., Sana & Evans 2011; Moe & Di Stefano 2017). The O-star binaries initially followed the observed orbital-period distribution of Sana & Evans (2011) and a uniform mass-ratio distribution.

The model clusters were evolved with the star-by-star, direct N-body evolution code NBODY7 (Aarseth 2012), which has been updated in several astrophysical aspects as detailed in Banerjee et al. (2020); Banerjee (2021a). The primary ‘engine’ for stellar and binary evolution in NBODY7 is BSE (Hurley et al. 2000, 2002) and that for post-Newtonian (PN) evolution of compact binaries and higher order systems is ARCHAIN (Mikkola & Tanikawa 1999; Mikkola & Merritt 2008). In Ba22, the ‘F12-rapid+B16-PPSN/PSN’ (Fryer et al. 2012; Belczynski et al. 2016; Banerjee et al. 2020) remnant-mass prescription was applied.

As detailed in Ba22 and Banerjee (2021b), the above set of evolutionary YMC models was then utilized to perform a ‘cluster population synthesis’. This provided estimates for present-day, intrinsic population properties of merging BBHs (and other compact-binaries) from YMCs of the Universe. In this population analysis, a power-law cluster birth mass function with index $\alpha = -2$ and the cosmic star formation rate evolution of Madau & Fragos (2017) were adopted. Although in Ba22 the ‘moderate-Z’ metallicity-redshift dependence of Chruslinska & Nelemans (2019) were adopted, here we repeat the cluster population synthesis exercise with the Madau & Fragos (2017) cosmic mean metallicity evolution with a Gaussian spread of 0.5 dex, as in Belczynski et al. (2020). This revised analysis ensures a proper correspondence with the isolated-binary evolutionary models used in this work (Sec. 2.1), in terms of cosmological ingredients. All results described in this paper correspond to this updated YMC BBH-merger population.

2.3. Modelling spin-orbit misalignment of merging binary black holes

Natal BH spins in isolated binary systems are derived under the assumption of effective angular momentum transport in massive stars, driven by the classic Tayler-Spruit dynamo Spruit (2002). We adopt BH spin magnitudes being fitted to the final angular momentum of massive stellar cores (see Belczynski et al. 2020), calculated using the MESA stellar evolutionary code (Paxton et al. 2015). Such BH natal spins (Kerr parameters) take values in the range $a \in 0.05 - 0.15$. As demonstrated in Belczynski et al. (2020), the BH natal spins are nearly independent of the progenitor stars’ initial spins. We allow for an efficient tidal spin-up of Wolf-Rayet (WR) stars in tight BH-WR and WR-WR binary systems, which may significantly increase the spin, usually of the second-born BH. For such spun-up BHs, we adopt the BH spin magnitude as in Eqn. 15 of Belczynski et al. (2020) for the systems with an orbital period in the range $P_{\text{orb}} = 0.1 - 1.3$ d and the maximum spin value of $a = 1$ for $P_{\text{orb}} < 0.1$ d. As explained in Belczynski et al. (2020), this ‘spun-up’ spin magnitude represents an upper limit. BH spins may also be slightly increased due to accretion in binary systems (King et al. 2001; Mondal et al. 2020). The misalignment angles of the two BH spin vectors with respect to the orbital angular momentum is derived as described in Sec. 2.2 of Belczynski et al. (2020). The initial spins of the ZAMS stars are fully aligned with their binary orbital angular momentum. The orbit and its spatial orientation may change due to the obtained natal kick and is calculated after both BHs formation. The individual BH misalignment

angles may differ due to the spin precession of binary components. We do not assume possible BH spin alignment with orbital angular momentum due to tides or mass transfer. In this way, we expose the maximum effect of generating misalignment in BBH mergers for the adopted model of natal kicks.

As for the YMC models, simplistic schemes for distinguishing between non-spun-up BHs and spun-up BHs and between BBHs depending on the formation channel were adopted in Ba22 (see the paper for the details). Essentially, in these models, a BH is flagged as spun-up if, after formation, it undergoes matter accretion due to a BH-star merger or mass transfer in a binary or if it forms in a tidally-interacting binary. In this study, we reassign the BH spins and the BBH spin-orbit misalignment from the YMC models through post-processing as described below.

Such cluster models with primordial binaries yield two ‘types’ of merging BBHs. They are (a) dynamically assembled BBHs, where the member BHs form uncorrelated, *i.e.*, in different primordial binaries, in a binary formed via exchange encounter(s), or from single stars, and (b) primordially paired BBHs³, where the members derive from the same primordial binary. Due to the moderate escape speed of the clusters ($\sim 50 \text{ km s}^{-1}$), a merged BH typically gets ejected from such clusters right after the merger by the associated GW recoil. No hierarchical BBH merger occurred in these models.

The absence of hierarchical mergers, in turn, justifies post-processing of the YMC BBH-merger populations to explore different BH-spin and alignment models. At present, stellar-mass BHs’ spin magnitudes and their distribution are far from being robustly determined (from observed GW events or theoretical models). Therefore, inspired by results from observed events and theoretical works, we consider several possibilities for the YMC BHs’ spins. First, based on the bimodal BH-spin distribution as obtained from LVK’s latest population analyses (Abbott et al. 2023, their Fig. 17), natal spins (Kerr parameters) of the non-spun-up BHs are assigned randomly from a Maxwellian distribution peaked at $a_0 = 0.1$ and those of the spun-up BHs are chosen from a higher Maxwellian, peaked at $a_{\text{high}} = 0.33$. To explore uncertainties in the results, additional cases, namely, $a_{\text{high}} = 0.5$ and $a_{\text{high}} = a_0 = 0.1$ (no spin-up of BHs) are considered. Furthermore, we consider the χ_{eff} distribution due to the upper limit of WR spin-up,

³ Also referred to as ‘original’ BBHs by some authors, *e.g.*, Di Carlo et al. (2020).

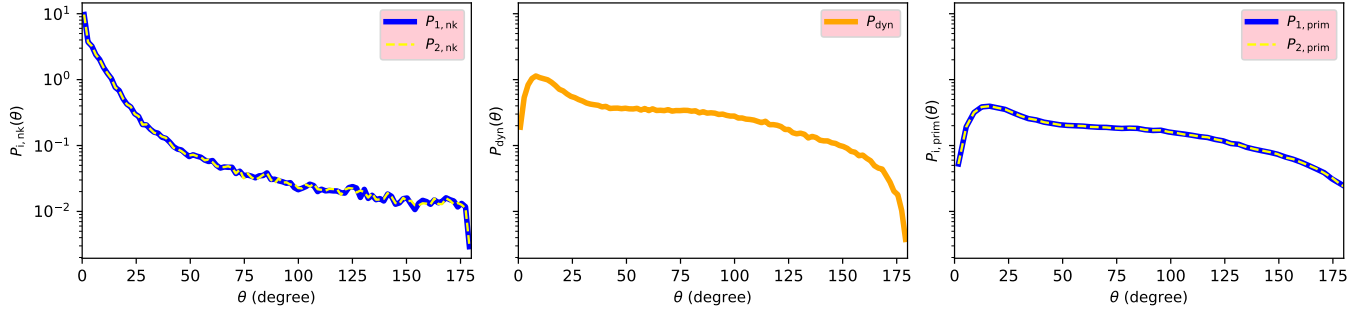


Figure 1. Probability density functions for spin-orbit misalignment angles of merging BBHs, due to natal kicks (left panel), binary-single dynamical interactions (middle), and the combination of these processes (right), as considered in this work. These PDFs correspond to present-day, intrinsic populations of merging BBHs.

as modelled in our isolated binary population (the **b'** populations; see below).

For dynamically assembled mergers from YMCs (hereafter subpopulation **b1**), as in Ba22, the involved BHs are assigned isotropic and independent spin orientations, *i.e.*,

$$\cos(\theta_{i,\text{iso}}) \in \mathcal{U}(-1, 1), \quad i = 1, 2. \quad (2)$$

Here $\mathcal{U}(-1, 1)$ represents a uniform probability distribution between $[-1, 1]$ ⁴.

As for primordially paired mergers (hereafter subpopulation **b2ymc**), the BBH would tend to be spin-orbit aligned due to (internal) binary interactions of the parent stellar binary. However, in general, the BBH won't be perfectly spin-orbit aligned due to (i) natal kicks of the BHs which are generally off the binary's orbital plane (see above) and (ii) misalignment introduced by dynamical encounters. In the YMC models, such natal-kick and 'dynamical' tilts were not explicitly considered during the N-body computations. In this study, we model the **b2ymc** tilt angles as described below.

For each event in the merging BBH population, the spin-orbit misalignment angle due to natal kick for both members are drawn independently from the CE21 (Sec. 2.1) tilt angle probability distribution:

$$\theta_{i,\text{nk}} \in P_{i,\text{nk}}(\theta), \quad i = 1, 2. \quad (3)$$

This import is consistent, since both the isolated binary and YMC models adopt the same fallback-modulated, momentum-conserving natal kick prescription (Belczynski et al. 2008; Fryer et al. 2012; Banerjee et al. 2020). Dynamical encounters will introduce a common extra tilt,

$$\theta_{\text{dyn}} \in P_{\text{dyn}}(\theta), \quad (4)$$

⁴ To facilitate such post-processing, the BBH-merger population from the cluster population synthesis (Sec. 2.2) are tagged, based on information from the original N-body simulations, to be dynamically assembled or primordially paired out of non-spun-up or spun-up members.

to both BHs. We estimate P_{dyn} from the numerical binary-single scattering experiments of Trani et al. (2021), which scatterings are close passages involving mainly resonant/chaotic interactions. In particular, the data corresponding to their Figure 2 is utilized to construct P_{dyn} (averaged over metallicities)⁵. Hence, the total spin-orbit misalignment angles of the merging components of a **b2ymc** BBH is (since the natal-kick and dynamical-encounter events would occur independently)⁶

$$\theta_{i,\text{prim}} = \theta_{i,\text{nk}} + \theta_{\text{dyn}}, \quad i = 1, 2. \quad (5)$$

Generally, $\theta_{i,\text{prim}}$ can be expected follow a probability distribution,

$$\theta_{i,\text{prim}} \in P_{i,\text{prim}}(\theta), \quad i = 1, 2, \quad (6)$$

which would be shallower than both $P_{i,\text{nk}}(\theta)$ and $P_{\text{dyn}}(\theta)$.

3. RESULTS

The probability density functions (PDF) $P_{i,\text{nk}}(\theta)$, $P_{\text{dyn}}(\theta)$, and $P_{i,\text{prim}}(\theta)$ are shown in Fig. 1. The figure demonstrates that the spin-orbit alignment of merging BBHs, derived from a population of isolated binaries, can deteriorate significantly but not completely if the binary population is subjected to dynamical binary-single interactions inside a cluster.

Fig. 2 shows the corresponding χ_{eff} probability density distributions for the **b1** and **b2ymc** subpopulations.

⁵ $P_{\text{dyn}}(\theta)$ represents the tilt angle distribution after a single encounter. However, a BBH may undergo multiple encounters inside a cluster until its in-cluster or ejected merger. Since the encounter events are practically mutually exclusive (one encounter occurs at a time except for very rare situations), $\theta_{\text{dyn}} \in \sum_{k=1}^n P_{\text{dyn}}(\theta) \propto P_{\text{dyn}}(\theta)$.

⁶ In their original references, both $P_{i,\text{nk}}(\theta)$ and $P_{\text{dyn}}(\theta)$ are defined over $0 \leq \theta \leq \pi$. In practice, $P_{\text{dyn}}(\theta)$ is extended by mirror-reflecting it over $\pi \leq \theta \leq 2\pi$. This effectively allows randomly adding or subtracting θ_{dyn} to/from $\theta_{i,\text{nk}}$.

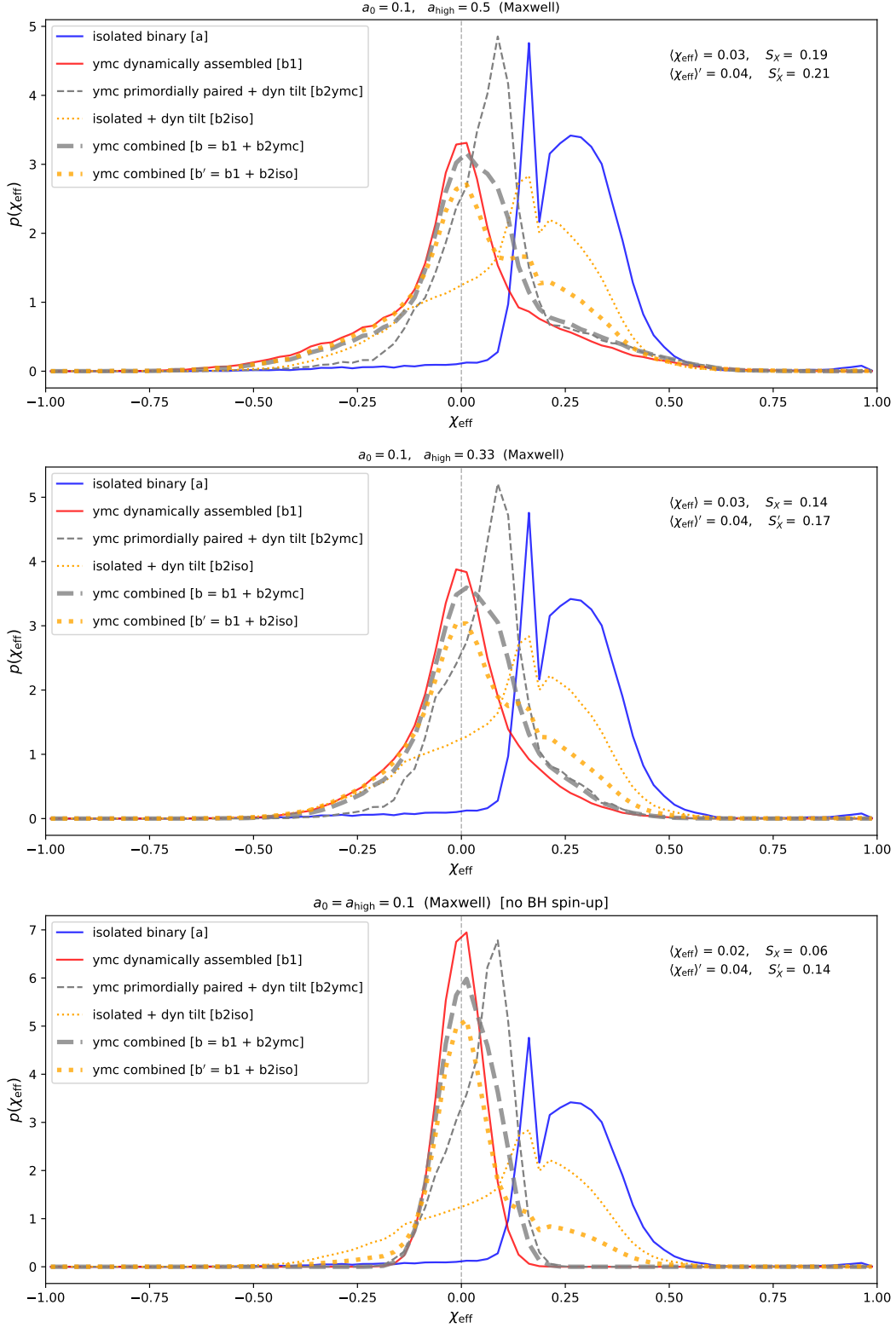


Figure 2. Present-day, intrinsic distributions of χ_{eff} , $p(\chi_{\text{eff}})$, for the merging BBH populations from YMCs and isolated binaries. For YMCs, the $p(\chi_{\text{eff}})$ of the dynamically assembled (b1) and primordially paired (b2ymc) subpopulations and as well as those of the combined populations (b and b') are shown separately. The transformation of the isolated-binary $p(\chi_{\text{eff}})$ due to dynamical interactions inside a cluster (*i.e.*, of population a to b2iso) is also demonstrated. While plotting, each of the $p(\chi_{\text{eff}})$ distribution is individually normalized to unity. The top (middle) panel corresponds to $a_{\text{high}} = 0.5$ (0.33) and the bottom panel corresponds to the case where accretion-induced spin-up of BHs is not allowed in the YMC models. The population means and standard deviations of χ_{eff} , corresponding to the combined distributions, are indicated in the upper-right corner of the respective panel. See text for further details.

The top and middle panel shows the case $a_{\text{high}} = 0.5$ and $a_{\text{high}} = 0.33$, respectively. The corresponding combined distribution, representing the overall χ_{eff} distribution of the observable merging BBH population from YMCs (hereafter population **b**), is shown. The panels also show how the χ_{eff} distribution from pure isolated binary evolution (*i.e.*, from population **a**; see above) would transform had these binaries been subjected to dynamical encounters inside a cluster (hereafter subpopulation **b2iso**), as well as the corresponding combined χ_{eff} distribution (hereafter population **b'**)⁷. Fig. 2 (bottom panel) shows the same distributions when *no* spin-up of a BH due to mass accretion or binary interaction is assumed for the YMC models, *i.e.*, all BHs have Kerr parameters drawn from a Maxwellian peaked at $a_0 = a_{\text{high}} = 0.1$.

The corresponding mean, $\langle\chi_{\text{eff}}\rangle$ ($\langle\chi_{\text{eff}}\rangle'$), and SD, S_X (S'_X), of population **b** (**b'**) are indicated on each panel of Fig. 2. The values of $\langle\chi_{\text{eff}}\rangle$ and S_X increase with increasing a_{high} . This is because, with increasing a_{high} , the peak of the **b2ymc** χ_{eff} distribution is shifted further towards $\chi_{\text{eff}} > 0$ and, at the same time, both **b1** and **b2ymc** distributions become wider. These behaviors simply follow from the definition of χ_{eff} (Eqn. 1) and the assignments of the BH Kerr parameters and tilt angles for the **b1** and **b2ymc** subpopulations (Sec. 2.3). The value of $\langle\chi_{\text{eff}}\rangle'$ is practically independent of a_{high} since the asymmetry in the **b'** χ_{eff} distribution stems from that of the **b2iso** subpopulation. Subpopulation **b2iso** is derived by applying only dynamical tilts to population **a** and hence is independent of the choice of a_{high} . The weak dependence of S'_X on a_{high} is due to the mixing of the (symmetric) **b1** subpopulation into population **b'**, **b1** being a_{high} -dependent (Sec. 2.3).

Table 1 shows the means, SDs, and percentages of $\chi_{\text{eff}} < 0$ mergers for all the individual χ_{eff} distributions shown in Fig. 2. For comparison, the corresponding LVK values are shown in the table as well (see Secs. 1 and 4 for a discussion). The LVK-observed values are obtained from the GWTC-3 public data, utilizing the stacked $p(\chi_{\text{eff}})$ distributions (500 of them) as read by the supplied script `make_gaussian_chi_eff.py`. These $p(\chi_{\text{eff}})$ distributions comprise the data underlying Fig. 16 (left panel) of Abbott et al. (2023) and are obtained by them based on their ‘Gaussian’ BH-spin population model. The set of $p(\chi_{\text{eff}})$ corresponds to sets of $\langle\chi_{\text{eff}}\rangle$, S_X , and f_{X-} values. In Table 1, the quoted LVK-observed values are the unweighted mean, 5th percentile, and 95th per-

centile of the corresponding value-set. (The unweighted means are very close to the corresponding median or 50th-percentile values.)

The χ_{eff} distributions of the combined YMC BBH-merger population (**b** and **b'**), overall, appear similar to the observed χ_{eff} distribution. Nevertheless, these computed populations have mean values that are somewhat smaller than the LVK’s mean χ_{eff} (Sec. 1) and they have negative χ_{eff} fractions ($f_{X-} \approx f'_{X-} \approx 41\%$; see Table 1) somewhat higher than that of the observed BBH-merger population. Given the rather large SD values, such small χ_{eff} -asymmetries of the YMC BBH-merger population are still consistent with the observed asymmetry. In contrast, the χ_{eff} distribution of population **a** has a mean (an SD) of $\langle\chi_{\text{eff}}\rangle^a = 0.26$ ($S_X^a = 0.14$) and a negative- χ_{eff} -merger fraction of $f_{X-}^a = 3\%$. In other words, pure isolated binary evolution produces a χ_{eff} distribution that is significantly more asymmetric (aligned) than the observed χ_{eff} distribution.

The above results correspond to $P_{\text{i,nk}}$ due to the CE21 isolated binary evolution model. The RLOF21 (Sec. 2.1) counterparts are presented in Appendix A. As can be seen, $P_{\text{i,nk}}$ due to the RLOF21 isolated binary model leaves the results practically unaltered. For RLOF21, $\langle\chi_{\text{eff}}\rangle^a = 0.24$, $S_X^a = 0.18$, and $f_{X-}^a = 7\%$. In Appendix B, we demonstrate cases with further choices of BH spins. In particular, we limit a_0 and a_{high} to have the same ranges as in our isolated-binary model. As seen, the results do not alter much among these cases.

4. DISCUSSIONS AND OUTLOOK

In this study, we consider the χ_{eff} distributions of observable merging BBH populations produced by YMCs and isolated, massive stellar binaries of the Universe. Such model populations are obtained based on population synthesis of massive binaries (using `StarTrack`; Sec. 2.1) and direct N-body evolutionary models of YMCs (using `NBODY7`; Sec. 2.2). In our analysis, we take into account spin-orbit misalignments of the merging BBHs due to both natal kicks and dynamical encounters inside clusters (Sec. 2.3). We show that (Sec. 3) (i) a primordially paired merging BBH population from the YMC models introduces an asymmetry in the χ_{eff} distribution towards $\chi_{\text{eff}} > 0$, (ii) the overall bias of the YMC BBH-merger population towards aligned mergers ($\langle\chi_{\text{eff}}\rangle \leq 0.05$, $f_{X-} \approx 40\%$) is somewhat smaller than but still comparable to that in the observed BBH-merger population, and (iii) the χ_{eff} -asymmetry in BBH mergers from isolated binaries alone ($\langle\chi_{\text{eff}}\rangle^a \approx 0.2$,

⁷ In obtaining the **b'** population, subpopulations **b1** and **b2iso** are mixed in the same proportions as those of **b1** and **b2ymc** in population **b**.

Table 1. Statistics of the model χ_{eff} distributions.

Merging BBH population	$\langle\chi_{\text{eff}}\rangle$	S_X	$f_X -$
LVK observed	$0.06^{+0.03}_{-0.04}$	$0.11^{+0.04}_{-0.03}$	$28.32^{+14.46}_{-13.21}$
isolated binary [a]	0.26	0.14	2.83
isolated + dyn. tilt [b2iso]	0.12	0.19	25.32
$a_0 = 0.1, \quad a_{\text{high}} = 0.5$ (Maxwell)			
ymc combined [b = b1 + b2ymc]	0.03	0.19	40.69
ymc combined [b' = b1 + b2iso]	0.04	0.21	40.74
ymc dyn. assembled [b1]	0.00	0.20	50.19
ymc prim. paired + dyn. tilt [b2ymc]	0.08	0.15	25.10
$a_0 = 0.1, \quad a_{\text{high}} = 0.33$ (Maxwell)			
ymc combined [b = b1 + b2ymc]	0.03	0.14	40.80
ymc combined [b' = b1 + b2iso]	0.04	0.17	40.87
ymc dyn. assembled [b1]	0.00	0.14	50.38
ymc prim. paired + dyn. tilt [b2ymc]	0.07	0.11	25.43
$a_0 = a_{\text{high}} = 0.1$ (Maxwell) [no BH spin-up]			
ymc combined [b = b1 + b2ymc]	0.02	0.06	40.60
ymc combined [b' = b1 + b2iso]	0.04	0.14	40.66
ymc dyn. assembled [b1]	0.00	0.05	49.95
ymc prim. paired + dyn. tilt [b2ymc]	0.05	0.07	24.78

NOTE—The columns from left to right are, respectively, BBH-merger population type, mean of the population’s χ_{eff} distribution, standard deviation of the χ_{eff} distribution, and percentage of events in the population with $\chi_{\text{eff}} < 0$. The LVK-observed values (see text) are the mean values along with the 90% confidence limits. The YMC-population values for different a_{high} (Sec. 2.3; Fig. 2) are shown in separate sections, as indicated.

$f_X^a - \leq 7\%$) is rather high compared to that in the observed population.

Among stellar clusters, young clusters such as YMCs would have the highest contribution towards primordially paired GR mergers, since such mergers have short delay times ($\lesssim 100$ Myr). With time, dynamically paired mergers become increasingly dominant in clusters (see Belczynski et al. 2022a and references therein). Hence, old clusters (*e.g.*, old open clusters, globular clusters, nuclear clusters) are unlikely to cause an alignment bias in BBH mergers. The above results and considerations suggest that a combination of cluster and isolated-binary merger channels across cosmic time might yield the observed χ_{eff} asymmetry. This possibility can be explored by a straightforward extension of the approach described in Banerjee (2022b), which will be taken up in future work. The method would as well allow incorporating other promising channels for orientation bias in BBH mergers such as dynamics in AGN gas disks (Wang et al. 2021; Rozner et al. 2022).

The extent of the contribution of young clusters to the observed BBH-merger the population is, at present, far

from being settled. This stems from various astrophysical and as well GW-observational uncertainties; see, *e.g.*, Antonini & Gieles (2020); Banerjee (2020, 2021b, 2022b); Chattopadhyay et al. (2022). The same is true for other dynamical channels (*e.g.*, Chatterjee et al. 2017; Arca Sedda et al. 2020) and the isolated-binary channel (*e.g.*, van Son et al. 2022; Belczynski et al. 2022b). With further GW events detected during the forthcoming observing runs, constraints on the different channels can be expected to improve.

In this work, we present the results of one physical model (CE21) for the isolated binary evolution channel, where the vast majority of BBH mergers (over 90% of them) form via CE evolution scenario. In Appendix A, we provide additional results for the second, RLOF21 model, which corresponds to much more restrictive CE development criteria than the ones applied for the CE21 model. The revised criteria, motivated by the studies of Pavlovskii et al. (2017), change the dominant formation scenario for the BBH mergers which, instead of CE, now consists of a stable mass transfer phase ($\sim 90\%$ of systems) during the second RLOF. This modification also

significantly reduces BBH merger rates at high redshifts ($z > 1.0$), since the produced BBH systems tend to have wider orbital separations (also longer delay times) than those in the CE scenario, see, *e.g.*, Figure B1 in [Olejak et al. \(2022\)](#).

Unexpectedly, the two tested models, which might be considered as extremes of the CE development criteria, result in similar distributions of the χ_{eff} . A significant fraction of high-spinning BBH mergers in model RLOF21 originates from a mass-reversal scenario, that includes two episodes of stable mass transfer [Olejak & Belczynski \(2021\)](#). However, note that similar studies, which apply CE development criteria with restrictions somewhere between our CE21 and RLOF21 models, may lead to other findings and conclusions. For example, [Zevin & Bavera \(2022\)](#) and [Bavera et al. \(2022\)](#) find that the stable mass transfer formation scenario tends to produce lower χ_{eff} s than in CE evolution. The discrepancy between our findings and theirs is caused by the absence of our mass-reversal evolutionary scenario in their simulations. Instead, this scenario is common in our simulations due to the restrictive CE development criteria, allowing highly unequal mass systems (with the donor to BH mass ratio $\gtrsim 6$) to avoid CE phase evolution [Olejak & Belczynski \(2021\)](#). Note that, *e.g.*, [Broekgaarden et al. \(2022\)](#) also proposed a mass-reversal scenario (via stable mass transfer) as a possible formation channel for a BBH merger with a non-negligible χ_{eff} value. See Appendix A for more details.

Our studies test only two models for isolated binary evolution channel which result in a similar distribution of χ_{eff} , but a significant difference in the distribution of individual BH spin magnitudes, see Appendix A and [Olejak & Belczynski \(2021\)](#) for details. Besides criteria for CE development, there are many other unconstrained physical processes and parameters in rapid population synthesis codes. Some broader parameter studies, testing how different assumptions on, *e.g.*, angular momentum transport, increased accretion rate, or CE efficiency in parameterized α_{CE} formalism impact the fraction of high-spinning BBH mergers in isolated binary evolution in CE and stable mass transfer scenarios, may be found in [van Son et al. \(2020\)](#); [Zevin & Bavera \(2022\)](#); [Broekgaarden et al. \(2022\)](#) and [Carole et al. \(2023\)](#). A few other examples of uncertainties that may affect effective spins of BBH mergers in isolated binary evolution but has not been examined within this study are: metallicity-specific star formation rate density ([Santoliquido et al. 2021](#); [Briel et al. 2021](#); [Chruslińska 2022](#)), stellar winds ([Vink et al. 2001](#); [Sander et al. 2022](#)), core-collapse SN mechanism ([Sukhbold et al. 2016](#); [Fryer et al. 2022](#); [Olejak et al.](#)

[2022](#); [Shao 2022](#)) and BH natal kicks ([Mandel et al. 2021](#)).

In fact, it may even be possible to reproduce the observed χ_{eff} distribution by the isolated binary evolution channel alone. Especially, our calculations of WR tidal spin-up should be considered as an upper limit ([Belczynski et al. 2020](#); [Ma & Fuller 2023](#)) that may lead to a significant overestimation of the fraction of high- χ_{eff} BBH mergers. Assumptions about poorly understood BH natal kicks affect the spin-orbital misalignment, and thus the fraction of BBHs with negative χ_{eff} – larger kicks would produce a larger fraction of negative- χ_{eff} mergers from binary evolution, *e.g.*, [Belczynski et al. \(2020\)](#). Also, the dynamo of [Fuller & Ma \(2019\)](#), rather than the presently used Tayler-Spruit dynamo, along with less efficient tidal spin-up of WR stars [Ma & Fuller \(2023\)](#) would move the peak of the isolated-binary χ_{eff} distribution towards a smaller value.

It is worth noting that our isolated-binary evolutionary model does not incorporate chemically homogeneous binary evolution. Adequately tight and massive binaries can undergo chemically homogeneous evolution, which would result in highly spinning, near equal mass, fully aligned BBH mergers and hence contribute towards enhancing the positive χ_{eff} bias in isolated-binary BBH mergers. The chemically homogeneous evolution scenario ([De Mink et al. 2009](#); [de Mink et al. 2010](#); [Marchant et al. 2016](#); [De Mink & Mandel 2016](#); [Mandel 2016](#); [Riley et al. 2021](#)) applies to initially tight, almost contact, massive binary systems with their periods below $P < 2$ days ([De Mink & Mandel 2016](#)). Main sequence components get tidally spun up, which induces efficient mixing from the interior throughout their envelope, providing the core with additional nuclear-burning elements. Importantly, the rapid rotation of stars and the efficient mixing is expected to result in a significant decrease in radius expansion in contrast to the non-rotating evolutionary models ([Maeder 1987](#)). That allows components to avoid the stellar merger after the completion of hydrogen burning and survive as a tight binary system ([Nelson & Eggleton 2001](#)). The chemically homogeneous formation scenario favors massive BBH mergers of the total mass of $M_{\text{tot}} \in 50 - 110 M_{\odot}$ with secondary to primary BH mass ratio of $q \gtrsim 0.8$ ([Marchant et al. 2016](#); [De Mink & Mandel 2016](#)).

In this work, we focus only on the χ_{eff} parameter distribution of the detected BBH mergers. However, LVK also provides distributions of other compact-object parameters, *e.g.*, masses, mass ratio, and as well reports potential correlations between mass ratio and χ_{eff} of BBH mergers ([Abbott et al. 2023](#)). Further studies

need to be done to reconstruct all properties of the GW-source population.

The present YMC model set from Ba22 (Sec. 2.2) has only one representative initial cluster mass and size (although it spans over a wide range of metallicity), which is a limitation of the model grid. A grid spanning over cluster mass and size is being computed which will eventually be incorporated. Although the cluster model grid of Banerjee (2021a) spans over cluster mass, size, and metallicity, the model grid of Ba22 is preferred in the present analysis due to the latter grid’s homogeneity in properties. This ensures that no asymmetry occurs in the model BBH population due to artefacts of the cluster model grid.

Exploration of cluster parameters is important for an in-depth understanding of the production of primordially paired mergers in clusters. The relative numbers of primordially paired and dynamically assembled mergers directly influence the results of this work – a higher relative number of dynamical mergers would cause a more symmetric χ_{eff} distribution. Therefore, the initial fraction of primordial binaries among the BH-progenitor stars assumed in YMC models (which is 100% in the present models; see Sec. 2.2) would influence the resulting χ_{eff} distribution. Cluster (initial) density can play a more subtle role: on one hand, a denser cluster can more efficiently dynamically harden wide primordially paired (as well as dynamically assembled) BBHs and aid them in merging. On the other hand, higher density can also aid primordial binaries to undergo premature star-star mergers (via dynamical hardening or hierarchy formation), reducing the number of primordial BBH mergers. Initial orbital period distribution of the primordial binaries can similarly influence the primordially paired BBH merger fraction. In fact, a higher primordial binary fraction can trigger more frequent stellar-phase mergers of primordial binaries via binary-binary interactions that form hierarchical subsystems (*e.g.*, Geller et al. 2013), that way potentially weaken the dependence on primordial binary fraction. At present, how cluster parameters and stellar content influence the χ_{eff} distribution of BBH mergers from clusters is hardly explored and remains mainly an open question.

The present analysis does not identify instances where the dynamical assembly of the binary happens before the formation of the member BHs and hence, due to a potential interacting-binary phase, preferential alignment can be expected. This would boost the asymmetry in the YMC BBH mergers. This effect is unlikely to be critical for the presently considered pc-scale, massive clusters (although it will be modelled in future studies) where only the most massive members can mass-segregate over

the first $\lesssim 10$ Myr. However, early dynamical pairing among massive stars (via exchange and/or three-body encounters) is much more efficient in compact, low-mass clusters (of ~ 0.1 pc, $10^2 - 10^3 M_{\odot}$ initially) with short relaxation/mass-segregation time (*e.g.*, Di Carlo et al. 2020; Kumamoto et al. 2020; Rastello et al. 2021). Another limitation of the present analysis is that tilt due to binary-binary (and higher-order) encounters is not incorporated. Such encounters, although are generally less frequent than binary-single interactions, can potentially cause larger tilts (due to longer chaotic phase and more diverse outcomes) and hence enhance the randomization of the primordially paired BBHs’ orientations.

The comparison with the observed BBH-merger population, especially of negative χ_{eff} fraction (f_{X-}), should be taken with caution, given the former, alternative interpretation that the observed population is practically devoid of negative- χ_{eff} events (Roulet et al. 2021; Galadage et al. 2021). Notably, such interpretation, performed for the previous GW events catalog (not including the full O3 run), relies on the assumption of a significant contribution from a zero-spin BBH merger subpopulation. This assumption rests essentially on a specific, highly efficient (driven by modified Tayler-Spruit dynamo) stellar angular momentum transport model (Fuller & Ma 2019). A more recent, parameter-free analysis finds the distribution of BH spin magnitudes unimodal and concentrated at small but non-zero values (Callister & Farr 2023). Such distribution is more in line with the stellar models that apply the classic Tayler-Spruit dynamo (Spruit 2002; Belczynski et al. 2020). Hence, the interpretation by LVK leading to a finite f_{X-} without a zero-spin-merger ‘spike’ in the population (see Secs. 1, 3; Table 1), as adopted here, is, potentially, more general and model-inclusive.

Neither the isolated-binary nor the YMC models in the present study properly reproduces the observed χ_{eff} distribution of BBH mergers. However, the YMC χ_{eff} distribution is reasonably similar to the observed χ_{eff} distribution, taking into account the observational uncertainties. Given the observational and model uncertainties, at present it cannot be conclusively said whether one channel or a combination of channels causes the observed χ_{eff} distribution. This can be expected to be better settled only with further extensive model explorations and GW event detections.

We thank Alessandro A. Trani for providing the data corresponding to Figure 2 of their Trani et al. (2021) paper. Special thanks goes to tens of thousands of citizen-science project "Universe@home" (universeathome.pl) enthusiasts that help to develop the StarTrack population synthesis code used in this study. S.B. acknowledges funding for this work by the Deutsche Forschungsgemeinschaft (DFG, German Research Foundation) through the project "The dynamics of stellar-mass black holes in dense stellar systems and their role in gravitational-wave generation" (project number 405620641; PI: S. Banerjee). S.B. acknowledges the generous support and efficient system maintenance of the computing teams at the AIfA and HISKP. AO and KB acknowledge support from the Polish National Science Center (NCN) grant Maestro (2018/30/A/ST9/00050). AO is also supported by the Foundation for Polish Science (FNP) and a scholarship of the Minister of Education and Science (Poland).

Software: StarTrack (Belczynski et al. 2008), NBODY7 (Aarseth 2012), NumPy (Harris et al. 2020), matplotlib (Hunter 2007)

APPENDIX

A. THE CASE OF STABLE-RLOF-DOMINATED MERGING BBH FORMATION FROM ISOLATED BINARY EVOLUTION

The distributions of effective spin parameter derived for both tested CE development criteria, the less (CE21) and the more (RLOF21) restrictive, look similar. However, there is an important difference in the high-spinning BBH subpopulation between the CE and stable mass transfer formation scenarios Olejak & Belczynski (2021). Once we adopt the less restrictive criteria (CE21), for which BBH mergers are formed mainly via CE evolution, the second-born and tidally spun-up BH is usually the less massive one. It is also possible that systems with almost equal-mass components pass through a close WR-WR phase, during which both components are spun up; see Figure 2 of Olejak & Belczynski (2021).

Conversely, for the restrictive CE development criteria (RLOF21), the vast majority of BBH mergers form through stable mass transfer, and the second-born tidally spun-up BH is usually the more massive one. This result is common for this formation channel of highly-spinning BBH mergers via the mass-reversal scenario; see Figure 1 of Olejak & Belczynski (2021). Stable mass transfer, widely adopted by rapid population synthesis codes, is much less efficient in tightening the orbit than CE evolution. Therefore, our simulations require highly unequal mass ratio components at the onset of the second RLOF to eject enough mass and angular momentum for shortening the binary orbital period below $P \leq 1.3$ day and entering the WR tidal spin-up regime (Belczynski et al. 2020). This also results in the characteristic mass ratio distribution of BBH mergers formed via stable mass transfer channel (Olejak et al. 2021) which possesses a high, extensive peak between $q \approx 0.4 - 0.7$.

For this reason, the formation of a significant fraction of close BH-WR star systems via stable mass transfer is possible only while adopting very restrictive CE development criteria, which allows highly unequal mass systems, such with the donor to BH mass ratio $\frac{M_{\text{don}}}{M_{\text{BH}}} \gtrsim 6$, to go through stable mass transfer phase instead of CE. As our restrictive criteria are rather extreme among rapid population synthesis codes, such a mass-reversal formation scenario for high-spinning BBH mergers is unique for StarTrack code. However, see also the results of Broekgaarden et al. (2022) who also find the mass-reversal scenario as a possible origin of BBH mergers with non-negligible χ_{eff} .

Note that e.g., Zevin & Bavera (2022); Bavera et al. (2022) came to different conclusions, suggesting that once adopting effective angular momentum transport and Eddington-limited accretion, the fraction of high-spin BHs originating from a stable mass transfer channel should be smaller than for CE scenario due to the less efficient orbital tightening. In our StarTrack simulations, the stable mass transfer scenario also tends to produce wider systems than

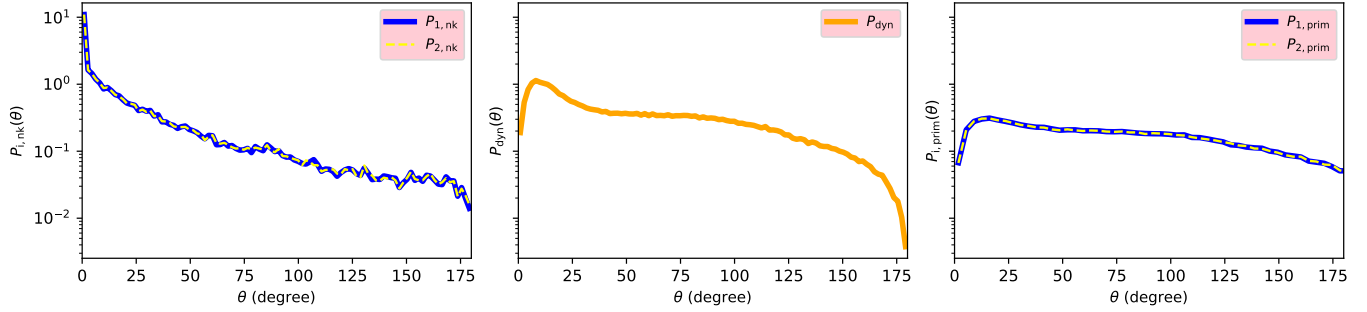


Figure 3. Same description as in Fig. 1 applies, except that the model isolated-binary population evolution forms BBH mergers primarily via stable RLOF (the RLOF21 model).

Table 2. Statistics of the model χ_{eff} distributions for the RLOF21 isolated binary model.

Population	$\langle \chi_{\text{eff}} \rangle$	S_X	$f_X -$
LVK observed	$0.06^{+0.03}_{-0.04}$	$0.11^{+0.04}_{-0.03}$	$28.32^{+14.46}_{-13.21}$
isolated [a]	0.24	0.18	7.52
isolated + dyn. tilt [b2iso]	0.11	0.22	28.39
$a_0 = 0.1, \quad a_{\text{high}} = 0.5$ (Maxwell)			
ymc combined [b = b1 + b2ymc]	0.03	0.19	41.34
ymc combined [b' = b1 + b2iso]	0.04	0.22	41.73
ymc dyn. assembled [b1]	0.00	0.20	49.85
ymc prim. paired + dyn. tilt [b2ymc]	0.07	0.15	27.60
$a_0 = 0.1, \quad a_{\text{high}} = 0.33$ (Maxwell)			
ymc combined [b = b1 + b2ymc]	0.02	0.13	41.40
ymc combined [b' = b1 + b2iso]	0.04	0.18	41.75
ymc dyn. assembled [b1]	0.00	0.14	49.82
ymc prim. paired + dyn. tilt [b2ymc]	0.06	0.11	27.64
$a_0 = a_{\text{high}} = 0.1$ (Maxwell) [no BH spin-up]			
ymc combined [b = b1 + b2ymc]	0.02	0.06	41.31
ymc combined [b' = b1 + b2iso]	0.04	0.15	41.88
ymc dyn. assembled [b1]	0.00	0.05	50.05
ymc prim. paired + dyn. tilt [b2ymc]	0.04	0.07	26.08

NOTE—The same description as in Table 1 applies.

evolution via CE, resulting in larger time delays and decreased BBH merger rates at higher redshifts, see e.g., Figure B1 in [Olejak et al. \(2022\)](#). The inconsistency between our results and those of other groups likely originates from the difference in the adopted CE development combined with a conservative assumption on angular momentum loss ([Olejak & Belczynski 2021](#)). Less restrictive criteria would eliminate the main formation scenario for high-spinning BHs via stable mass transfer found in our simulations, as highly unequal binaries would develop CE instead.

Figs. 3 and 4 and Table 2 show the results corresponding to the RLOF21 isolated binary evolution model (Sec. 2.1). The tilt-angle and χ_{eff} distributions and their mean values are close to those for the CE21 isolated binary evolution case (Sec. 2.1; Figs. 1 and 2).

B. RESULTS WITH ADDITIONAL BH-SPIN MODELS

In this section, we show additional cases based on the choice of BH spin. The cases are correspondingly de-

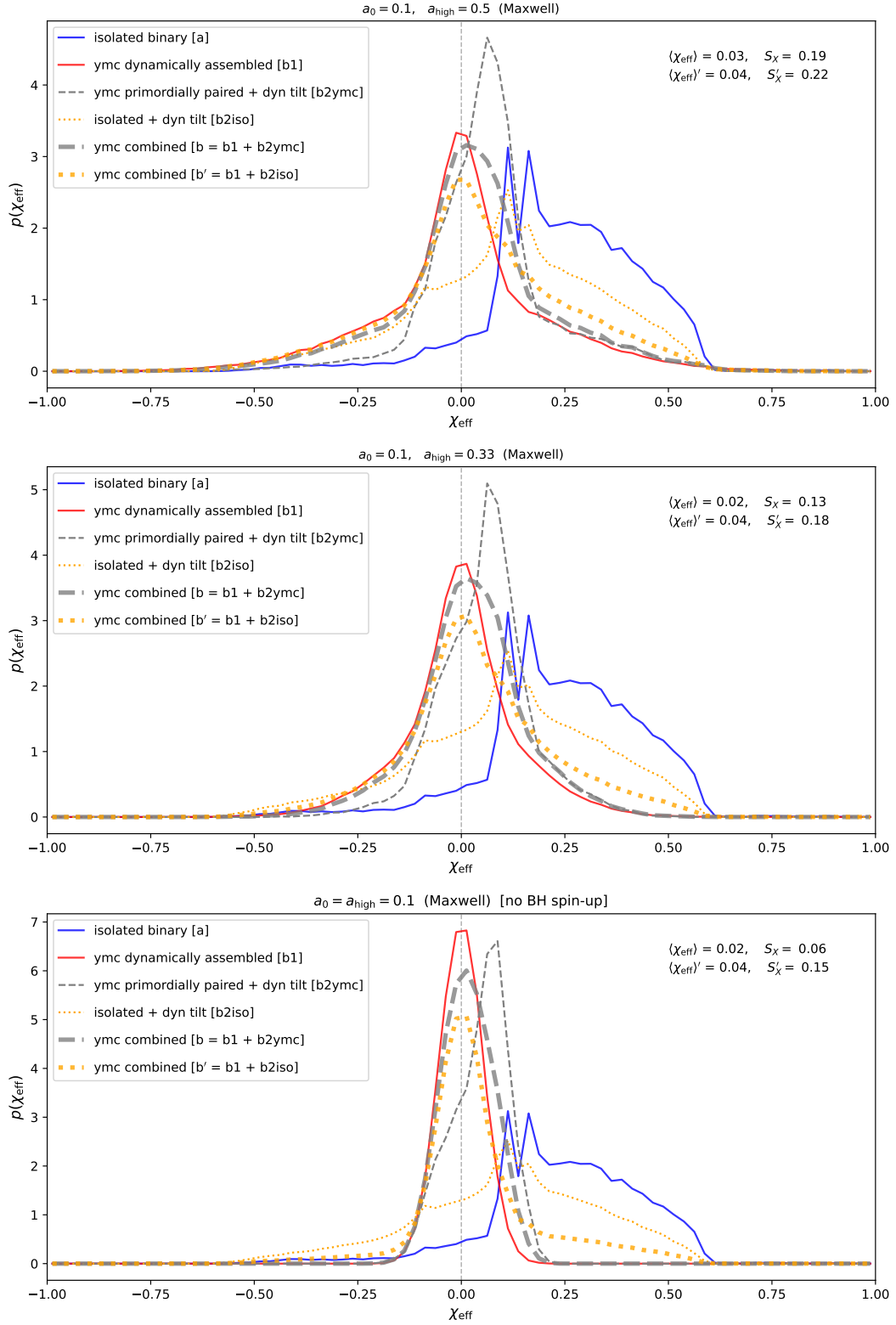


Figure 4. Same description as in Fig. 2 applies, except that the model isolated-binary population evolution forms BBH mergers primarily via stable RLOF (the RLOF21 model).

scribed in the caption of Figs. 5, 6 and 7. Overall, the distribution statistics for these cases are similar to those in Tables 1 and 2. In particular, $f_X - \approx 40\%$ in all cases.

For reference, the statistics corresponding to the distributions in Fig. 7 are provided in Table 3.

REFERENCES

- Aarseth, S. J. 2012, MNRAS, 422, 841, doi: [10.1111/j.1365-2966.2012.20666.x](https://doi.org/10.1111/j.1365-2966.2012.20666.x)
- Aasi, J., Abbott, B. P., Abbott, R., et al. 2015, Classical and Quantum Gravity, 32, 074001, doi: [10.1088/0264-9381/32/7/074001](https://doi.org/10.1088/0264-9381/32/7/074001)
- Abbott, B. P., Abbott, R., Abbott, T. D., et al. 2019, Physical Review X, 9, 031040, doi: [10.1103/PhysRevX.9.031040](https://doi.org/10.1103/PhysRevX.9.031040)
- Abbott, R., Abbott, T. D., Abraham, S., et al. 2021a, Phys. Rev. X, 11, 021053, doi: [10.1103/PhysRevX.11.021053](https://doi.org/10.1103/PhysRevX.11.021053)
- Abbott, R., Abbott, T. D., Acernese, F., et al. 2021b, arXiv e-prints, arXiv:2111.03606. <https://arxiv.org/abs/2111.03606>
- . 2021c, arXiv e-prints, arXiv:2108.01045. <https://arxiv.org/abs/2108.01045>
- . 2023, Physical Review X, 13, 011048, doi: [10.1103/PhysRevX.13.011048](https://doi.org/10.1103/PhysRevX.13.011048)
- Acernese, F., Agathos, M., Agatsuma, K., et al. 2015, Classical and Quantum Gravity, 32, 024001, doi: [10.1088/0264-9381/32/2/024001](https://doi.org/10.1088/0264-9381/32/2/024001)
- Ajith, P., Hannam, M., Husa, S., et al. 2011, Phys. Rev. Lett., 106, 241101, doi: [10.1103/PhysRevLett.106.241101](https://doi.org/10.1103/PhysRevLett.106.241101)
- Antonini, F., & Gieles, M. 2020, PhRvD, 102, 123016, doi: [10.1103/PhysRevD.102.123016](https://doi.org/10.1103/PhysRevD.102.123016)
- Arca Sedda, M., Mapelli, M., Benacquista, M., & Spera, M. 2021, arXiv e-prints, arXiv:2109.12119. <https://arxiv.org/abs/2109.12119>
- Arca Sedda, M., Mapelli, M., Spera, M., Benacquista, M., & Giacobbo, N. 2020, ApJ, 894, 133, doi: [10.3847/1538-4357/ab88b2](https://doi.org/10.3847/1538-4357/ab88b2)
- Banerjee, S. 2020, Phys. Rev. D, 102, 103002, doi: [10.1103/PhysRevD.102.103002](https://doi.org/10.1103/PhysRevD.102.103002)
- Banerjee, S. 2021a, MNRAS, 500, 3002, doi: [10.1093/mnras/staa2392](https://doi.org/10.1093/mnras/staa2392)
- . 2021b, MNRAS, 503, 3371, doi: [10.1093/mnras/stab591](https://doi.org/10.1093/mnras/stab591)
- . 2022a, A&A, 665, A20, doi: [10.1051/0004-6361/202142331](https://doi.org/10.1051/0004-6361/202142331)
- . 2022b, PhRvD, 105, 023004, doi: [10.1103/PhysRevD.105.023004](https://doi.org/10.1103/PhysRevD.105.023004)
- Banerjee, S., Belczynski, K., Fryer, C. L., et al. 2020, A&A, 639, A41, doi: [10.1051/0004-6361/201935332](https://doi.org/10.1051/0004-6361/201935332)
- Bavera, S. S., Fishbach, M., Zevin, M., Zapartas, E., & Fragos, T. 2022, A&A, 665, A59, doi: [10.1051/0004-6361/202243724](https://doi.org/10.1051/0004-6361/202243724)
- Belczynski, K., Doctor, Z., Zevin, M., et al. 2022a, ApJ, 935, 126, doi: [10.3847/1538-4357/ac8167](https://doi.org/10.3847/1538-4357/ac8167)
- Belczynski, K., Kalogera, V., Rasio, F. A., et al. 2008, The Astrophysical Journal Supplement Series, 174, 223, doi: [10.1086/521026](https://doi.org/10.1086/521026)
- Belczynski, K., Lorimer, D. R., Ridley, J. P., & Curran, S. J. 2010, MNRAS, 407, 1245, doi: [10.1111/j.1365-2966.2010.16970.x](https://doi.org/10.1111/j.1365-2966.2010.16970.x)
- Belczynski, K., Heger, A., Gladysz, W., et al. 2016, A&A, 594, A97, doi: [10.1051/0004-6361/201628980](https://doi.org/10.1051/0004-6361/201628980)
- Belczynski, K., Klencki, J., Fields, C. E., et al. 2020, A&A, 636, A104, doi: [10.1051/0004-6361/201936528](https://doi.org/10.1051/0004-6361/201936528)
- Belczynski, K., Romagnolo, A., Olejak, A., et al. 2022b, ApJ, 925, 69, doi: [10.3847/1538-4357/ac375a](https://doi.org/10.3847/1538-4357/ac375a)
- Branchesi, M. 2016, in Journal of Physics Conference Series, Vol. 718, Journal of Physics Conference Series, 022004, doi: [10.1088/1742-6596/718/2/022004](https://doi.org/10.1088/1742-6596/718/2/022004)
- Briel, M. M., Eldridge, J. J., Stanway, E. R., Stevance, H. F., & Chrimes, A. A. 2021, arXiv e-prints, arXiv:2111.08124. <https://arxiv.org/abs/2111.08124>
- Broekgaarden, F. S., Stevenson, S., & Thrane, E. 2022, ApJ, 938, 45, doi: [10.3847/1538-4357/ac8879](https://doi.org/10.3847/1538-4357/ac8879)
- Callister, T. A., & Farr, W. M. 2023, arXiv e-prints, arXiv:2302.07289, doi: [10.48550/arXiv.2302.07289](https://doi.org/10.48550/arXiv.2302.07289)
- Callister, T. A., Miller, S. J., Chatziioannou, K., & Farr, W. M. 2022, ApJL, 937, L13, doi: [10.3847/2041-8213/ac847e](https://doi.org/10.3847/2041-8213/ac847e)
- Carole, P., Michela, M., Filippo, S., Yann, B., & Roberta, R. 2023, arXiv e-prints, arXiv:2301.01312. <https://arxiv.org/abs/2301.01312>
- Chatterjee, S., Rodriguez, C. L., & Rasio, F. A. 2017, ApJ, 834, 68, doi: [10.3847/1538-4357/834/1/68](https://doi.org/10.3847/1538-4357/834/1/68)
- Chattopadhyay, D., Hurley, J., Stevenson, S., & Raidani, A. 2022, MNRAS, 513, 4527, doi: [10.1093/mnras/stac1163](https://doi.org/10.1093/mnras/stac1163)
- Chruślińska, M. 2022, arXiv e-prints, arXiv:2206.10622. <https://arxiv.org/abs/2206.10622>
- Chruslinska, M., & Nelemans, G. 2019, MNRAS, 488, 5300, doi: [10.1093/mnras/stz2057](https://doi.org/10.1093/mnras/stz2057)

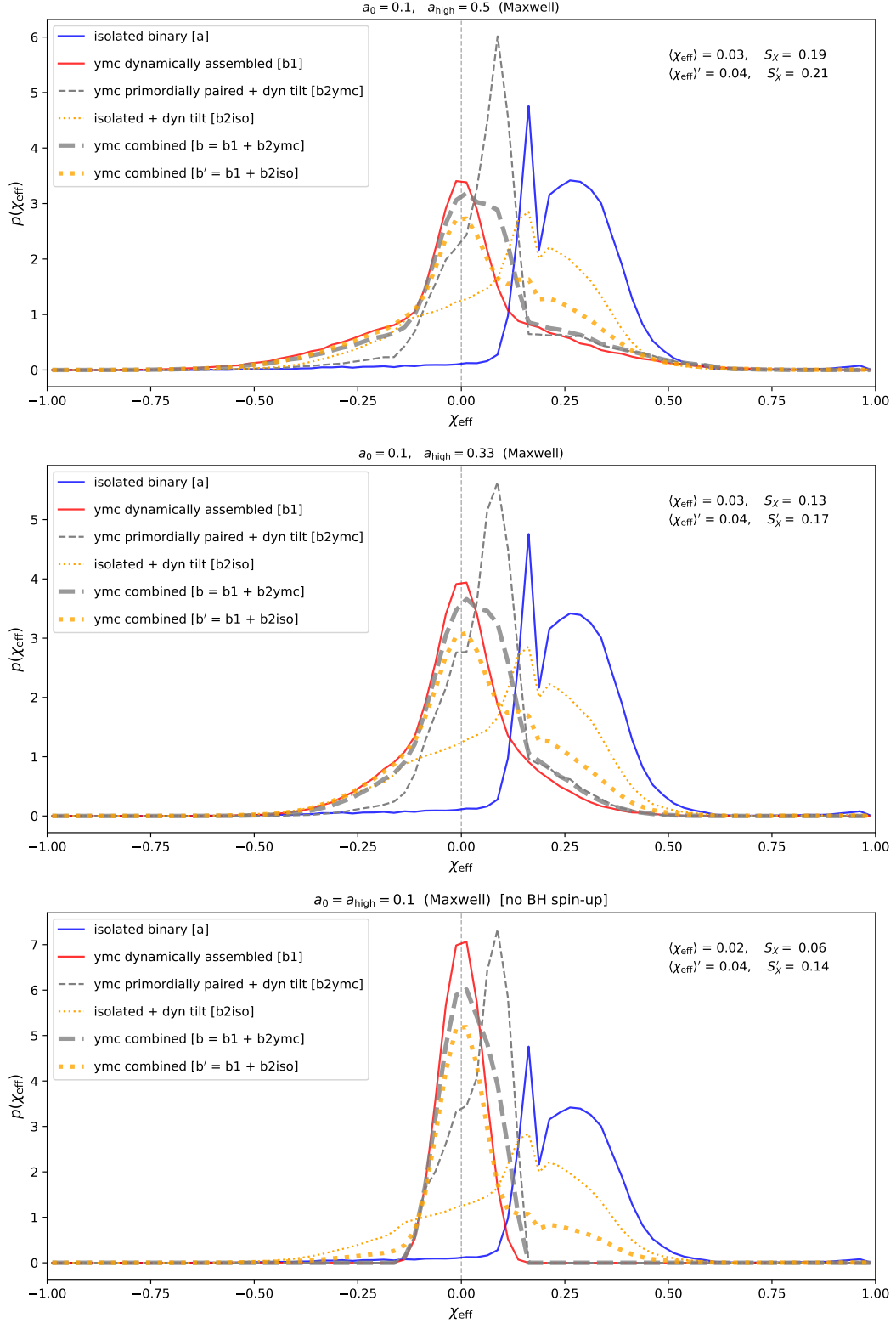


Figure 5. Same description as in Fig. 2 applies (the CE21 isolated-binary model), except that the base BH spin is truncated to be within $a_0 \in [0.05, 0.15]$. This truncation makes the range of a_0 consistent with that of [Belczynski et al. \(2020, their MESA model\)](#).

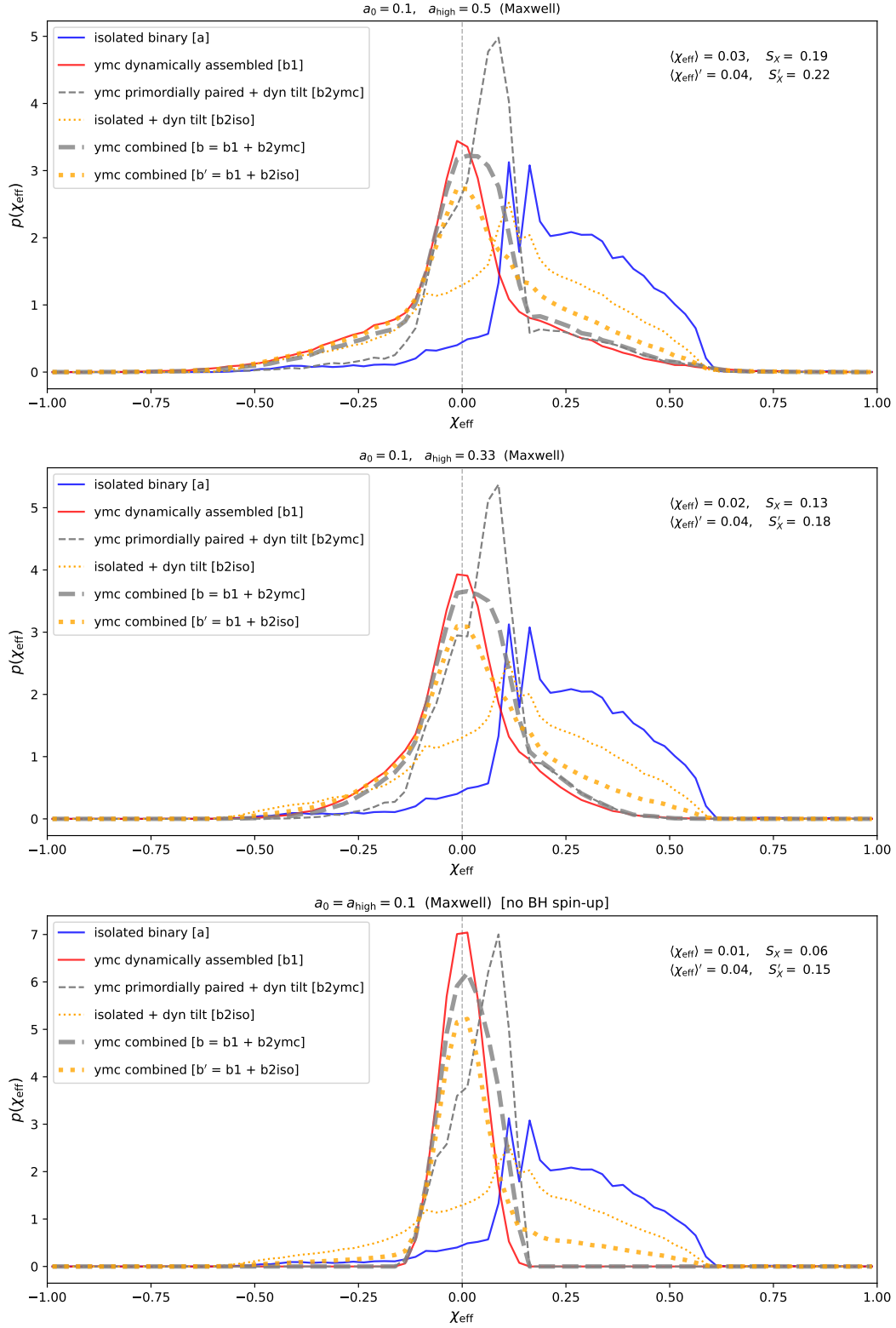


Figure 6. Same description as in Fig. 5 applies, except that the model isolated-binary population evolution forms BBH mergers primarily via stable RLOF (the RLOF21 model).

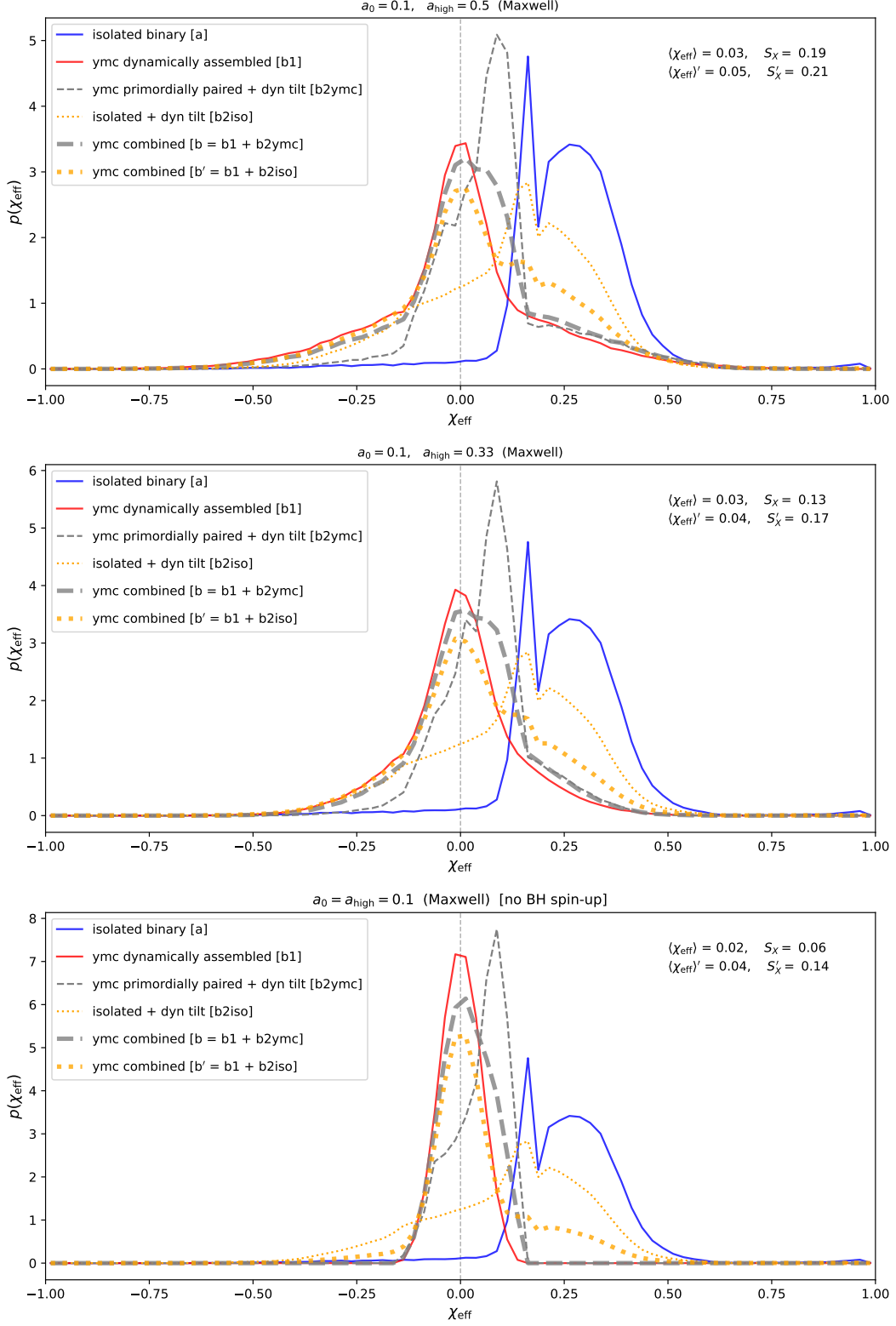


Figure 7. Same description as in Fig. 5 applies (the CE21 isolated-binary model), except that the spins of the spun-up BHs are truncated to be within $a_{\text{high}} \in [0.15, 1.0]$, in addition to $a_0 \in [0.05, 0.15]$. These truncations make the ranges of a_0 and a_{high} consistent with those of [Belczynski et al. \(2020\)](#).

Table 3. Statistics of the model χ_{eff} distributions corresponding to Fig. 7 (truncated a_0 and a_{high} ; CE21 isolated-binary model).

Population	$\langle\chi_{\text{eff}}\rangle$	S_X	f_X
LVK observed	$0.06^{+0.03}_{-0.04}$	$0.11^{+0.04}_{-0.03}$	$28.32^{+14.46}_{-13.21}$
isolated [a]	0.26	0.14	2.83
isolated + dyn. tilt [b2iso]	0.12	0.19	25.28
$a_0 = 0.1, \quad a_{\text{high}} = 0.5$ (Maxwell)			
ymc combined [$\mathbf{b} = \mathbf{b1} + \mathbf{b2ymc}$]	0.03	0.19	40.50
ymc combined [$\mathbf{b}' = \mathbf{b1} + \mathbf{b2iso}$]	0.05	0.21	40.65
ymc dyn. assembled [b1]	0.00	0.20	50.04
ymc prim. paired + dyn. tilt [b2ymc]	0.08	0.15	24.97
$a_0 = 0.1, \quad a_{\text{high}} = 0.33$ (Maxwell)			
ymc combined [$\mathbf{b} = \mathbf{b1} + \mathbf{b2ymc}$]	0.03	0.13	40.66
ymc combined [$\mathbf{b}' = \mathbf{b1} + \mathbf{b2iso}$]	0.04	0.17	40.82
ymc dyn. assembled [b1]	0.00	0.14	50.23
ymc prim. paired + dyn. tilt [b2ymc]	0.06	0.11	24.43
$a_0 = a_{\text{high}} = 0.1$ (Maxwell) [no BH spin-up]			
ymc combined [$\mathbf{b} = \mathbf{b1} + \mathbf{b2ymc}$]	0.02	0.06	40.46
ymc combined [$\mathbf{b}' = \mathbf{b1} + \mathbf{b2iso}$]	0.04	0.14	40.69
ymc dyn. assembled [b1]	0.00	0.05	50.09
ymc prim. paired + dyn. tilt [b2ymc]	0.05	0.06	24.55

NOTE—The same description as in Table 1 applies.

- de Mink, S. E., Cantiello, M., Langer, N., & Pols, O. R. 2010, in *American Institute of Physics Conference Series*, Vol. 1314, *International Conference on Binaries: in celebration of Ron Webbink's 65th Birthday*, ed. V. Kalogera & M. van der Sluys, 291–296, doi: [10.1063/1.3536387](https://doi.org/10.1063/1.3536387)
- De Mink, S. E., Cantiello, M., Langer, N., et al. 2009, *A&A*, 497, 243, doi: [10.1051/0004-6361/200811439](https://doi.org/10.1051/0004-6361/200811439)
- De Mink, S. E., & Mandel, I. 2016, *MNRAS*, 460, 3545, doi: [10.1093/mnras/stw1219](https://doi.org/10.1093/mnras/stw1219)
- Di Carlo, U. N., Mapelli, M., Giacobbo, N., et al. 2020, *MNRAS*, 498, 495, doi: [10.1093/mnras/staa2286](https://doi.org/10.1093/mnras/staa2286)
- Fryer, C. L., Belczynski, K., Wiktorowicz, G., et al. 2012, *ApJ*, 749, 91, doi: [10.1088/0004-637X/749/1/91](https://doi.org/10.1088/0004-637X/749/1/91)
- Fryer, C. L., Olejak, A., & Belczynski, K. 2022, *ApJ*, 931, 94, doi: [10.3847/1538-4357/ac6ac9](https://doi.org/10.3847/1538-4357/ac6ac9)
- Fuller, J., & Lu, W. 2022, *MNRAS*, 511, 3951, doi: [10.1093/mnras/stac317](https://doi.org/10.1093/mnras/stac317)
- Fuller, J., & Ma, L. 2019, *ApJL*, 881, L1, doi: [10.3847/2041-8213/ab339b](https://doi.org/10.3847/2041-8213/ab339b)
- Galadage, S., Talbot, C., Nagar, T., et al. 2021, *ApJL*, 921, L15, doi: [10.3847/2041-8213/ac2f3c](https://doi.org/10.3847/2041-8213/ac2f3c)
- Geller, A. M., Hurley, J. R., & Mathieu, R. D. 2013, *AJ*, 145, 8, doi: [10.1088/0004-6256/145/1/8](https://doi.org/10.1088/0004-6256/145/1/8)
- Gerosa, D., & Berti, E. 2017, *PhRvD*, 95, 124046, doi: [10.1103/PhysRevD.95.124046](https://doi.org/10.1103/PhysRevD.95.124046)
- Gerosa, D., & Fishbach, M. 2021, *Nature Astronomy*, 5, 749, doi: [10.1038/s41550-021-01398-w](https://doi.org/10.1038/s41550-021-01398-w)
- Harris, C. R., Millman, K. J., van der Walt, S. J., et al. 2020, *Nature*, 585, 357, doi: [10.1038/s41586-020-2649-2](https://doi.org/10.1038/s41586-020-2649-2)
- Hobbs, G., Lorimer, D. R., Lyne, A. G., & Kramer, M. 2005, *MNRAS*, 360, 974, doi: [10.1111/j.1365-2966.2005.09087.x](https://doi.org/10.1111/j.1365-2966.2005.09087.x)
- Hunter, J. D. 2007, *Computing in Science & Engineering*, 9, 90, doi: [10.1109/MCSE.2007.55](https://doi.org/10.1109/MCSE.2007.55)
- Hurley, J. R., Pols, O. R., & Tout, C. A. 2000, *Monthly Notices of the Royal Astronomical Society*, 315, 543, doi: [10.1046/j.1365-8711.2000.03426.x](https://doi.org/10.1046/j.1365-8711.2000.03426.x)
- Hurley, J. R., Tout, C. A., & Pols, O. R. 2002, *Monthly Notices of the Royal Astronomical Society*, 329, 897, doi: [10.1046/j.1365-8711.2002.05038.x](https://doi.org/10.1046/j.1365-8711.2002.05038.x)
- KAGRA Collaboration, Akutsu, T., Ando, M., et al. 2020, *Progress of Theoretical and Experimental Physics*, 2021, doi: [10.1093/ptep/ptaa120](https://doi.org/10.1093/ptep/ptaa120)
- King, A. R., Davies, M. B., Ward, M. J., Fabbiano, G., & Elvis, M. 2001, *ApJL*, 552, L109, doi: [10.1086/320343](https://doi.org/10.1086/320343)
- King, I. R. 1966, *AJ*, 71, 64, doi: [10.1086/109857](https://doi.org/10.1086/109857)
- Kroupa, P. 2001, *MNRAS*, 322, 231, doi: [10.1046/j.1365-8711.2001.04022.x](https://doi.org/10.1046/j.1365-8711.2001.04022.x)
- Krumholz, M. R., McKee, C. F., & Bland-Hawthorn, J. 2019, *ARA&A*, 57, 227, doi: [10.1146/annurev-astro-091918-104430](https://doi.org/10.1146/annurev-astro-091918-104430)
- Kumamoto, J., Fujii, M. S., & Tanikawa, A. 2020, *MNRAS*, 495, 4268, doi: [10.1093/mnras/staa1440](https://doi.org/10.1093/mnras/staa1440)
- Ma, L., & Fuller, J. 2023, *arXiv e-prints*, arXiv:2305.08356, doi: [10.48550/arXiv.2305.08356](https://doi.org/10.48550/arXiv.2305.08356)
- MacLeod, M., Macias, P., Ramirez-Ruiz, E., et al. 2017, *ApJ*, 835, 282, doi: [10.3847/1538-4357/835/2/282](https://doi.org/10.3847/1538-4357/835/2/282)
- Madau, P., & Fragos, T. 2017, *ApJ*, 840, 39, doi: [10.3847/1538-4357/aa6af9](https://doi.org/10.3847/1538-4357/aa6af9)
- Maeder, A. 1987, *A&A*, 178, 159
- Mandel, I. 2016, *MNRAS*, 456, 578, doi: [10.1093/mnras/stv2733](https://doi.org/10.1093/mnras/stv2733)
- Mandel, I., & Broekgaarden, F. S. 2022, *Living Reviews in Relativity*, 25, 1, doi: [10.1007/s41114-021-00034-3](https://doi.org/10.1007/s41114-021-00034-3)
- Mandel, I., Müller, B., Riley, J., et al. 2021, *MNRAS*, 500, 1380, doi: [10.1093/mnras/staa3390](https://doi.org/10.1093/mnras/staa3390)
- Mapelli, M. 2018, in *Journal of Physics Conference Series*, Vol. 957, *Journal of Physics Conference Series*, 012001, doi: [10.1088/1742-6596/957/1/012001](https://doi.org/10.1088/1742-6596/957/1/012001)
- Marchant, P., Langer, N., Podsiadlowski, P., Tauris, T. M., & Moriya, T. J. 2016, *A&A*, 588, A50, doi: [10.1051/0004-6361/201628133](https://doi.org/10.1051/0004-6361/201628133)
- Mészáros, P., Fox, D. B., Hanna, C., & Murase, K. 2019, *Nature Reviews Physics*, 1, 585, doi: [10.1038/s42254-019-0101-z](https://doi.org/10.1038/s42254-019-0101-z)
- Mikkola, S., & Merritt, D. 2008, *AJ*, 135, 2398, doi: [10.1088/0004-6256/135/6/2398](https://doi.org/10.1088/0004-6256/135/6/2398)
- Mikkola, S., & Tanikawa, K. 1999, *Monthly Notices of the Royal Astronomical Society*, 310, 745, doi: [10.1046/j.1365-8711.1999.02982.x](https://doi.org/10.1046/j.1365-8711.1999.02982.x)
- Moe, M., & Di Stefano, R. 2017, *ApJS*, 230, 15, doi: [10.3847/1538-4365/aa6fb6](https://doi.org/10.3847/1538-4365/aa6fb6)
- Mondal, S., Belczyński, K., Wiktorowicz, G., Lasota, J.-P., & King, A. R. 2020, *MNRAS*, 491, 2747, doi: [10.1093/mnras/stz3227](https://doi.org/10.1093/mnras/stz3227)
- Nelson, C. A., & Eggleton, P. P. 2001, *ApJ*, 552, 664, doi: [10.1086/320560](https://doi.org/10.1086/320560)
- Olejak, A., & Belczynski, K. 2021, *ApJL*, 921, L2, doi: [10.3847/2041-8213/ac2f48](https://doi.org/10.3847/2041-8213/ac2f48)
- Olejak, A., Belczynski, K., & Ivanova, N. 2021, *A&A*, 651, A100, doi: [10.1051/0004-6361/202140520](https://doi.org/10.1051/0004-6361/202140520)
- Olejak, A., Fryer, C. L., Belczynski, K., & Baibhav, V. 2022, *MNRAS*, 516, 2252, doi: [10.1093/mnras/stac2359](https://doi.org/10.1093/mnras/stac2359)
- Pavlovskii, K., Ivanova, N., Belczynski, K., & Van, K. X. 2017, *MNRAS*, 465, 2092, doi: [10.1093/mnras/stw2786](https://doi.org/10.1093/mnras/stw2786)
- Paxton, B., Marchant, P., Schwab, J., et al. 2015, *ApJS*, 220, 15, doi: [10.1088/0067-0049/220/1/15](https://doi.org/10.1088/0067-0049/220/1/15)

- Portegies Zwart, S. F., McMillan, S. L. W., & Gieles, M. 2010, *ARA&A*, 48, 431, doi: [10.1146/annurev-astro-081309-130834](https://doi.org/10.1146/annurev-astro-081309-130834)
- Rastello, S., Mapelli, M., Di Carlo, U. N., et al. 2021, *MNRAS*, 507, 3612, doi: [10.1093/mnras/stab2355](https://doi.org/10.1093/mnras/stab2355)
- Riley, J., Mandel, I., Marchant, P., et al. 2021, *MNRAS*, 505, 663, doi: [10.1093/mnras/stab1291](https://doi.org/10.1093/mnras/stab1291)
- Rodriguez, C. L., Amaro-Seoane, P., Chatterjee, S., & Rasio, F. A. 2018, *Phys. Rev. Lett.*, 120, 151101, doi: [10.1103/PhysRevLett.120.151101](https://doi.org/10.1103/PhysRevLett.120.151101)
- Roulet, J., Chia, H. S., Olsen, S., et al. 2021, *PhRvD*, 104, 083010, doi: [10.1103/PhysRevD.104.083010](https://doi.org/10.1103/PhysRevD.104.083010)
- Rozner, M., Generozov, A., & Perets, H. B. 2022, arXiv e-prints, arXiv:2212.00807. <https://arxiv.org/abs/2212.00807>
- Sana, H., & Evans, C. J. 2011, in *IAU Symposium*, Vol. 272, *Active OB Stars: Structure, Evolution, Mass Loss, and Critical Limits*, ed. C. Neiner, G. Wade, G. Meynet, & G. Peters, 474–485, doi: [10.1017/S1743921311011124](https://doi.org/10.1017/S1743921311011124)
- Sander, A. A. C., Vink, J. S., Higgins, E. R., et al. 2022, arXiv e-prints, arXiv:2202.04671. <https://arxiv.org/abs/2202.04671>
- Santoliquido, F., Mapelli, M., Giacobbo, N., Bouffanais, Y., & Artale, M. C. 2021, *MNRAS*, 502, 4877, doi: [10.1093/mnras/stab280](https://doi.org/10.1093/mnras/stab280)
- Shao, Y. 2022, *Research in Astronomy and Astrophysics*, 22, 122002, doi: [10.1088/1674-4527/ac995e](https://doi.org/10.1088/1674-4527/ac995e)
- Spera, M., Trani, A. A., & Mencagli, M. 2022, *Galaxies*, 10, 76, doi: [10.3390/galaxies10040076](https://doi.org/10.3390/galaxies10040076)
- Spruit, H. C. 2002, *A&A*, 381, 923, doi: [10.1051/0004-6361:20011465](https://doi.org/10.1051/0004-6361:20011465)
- Sukhbold, T., Ertl, T., Woosley, S. E., Brown, J. M., & Janka, H. T. 2016, *ApJ*, 821, 38, doi: [10.3847/0004-637X/821/1/38](https://doi.org/10.3847/0004-637X/821/1/38)
- Tauris, T. M. 2022, *ApJ*, 938, 66, doi: [10.3847/1538-4357/ac86c8](https://doi.org/10.3847/1538-4357/ac86c8)
- Trani, A. A., Tanikawa, A., Fujii, M. S., Leigh, N. W. C., & Kumamoto, J. 2021, *MNRAS*, 504, 910, doi: [10.1093/mnras/stab967](https://doi.org/10.1093/mnras/stab967)
- van Son, L. A. C., De Mink, S. E., Broekgaarden, F. S., et al. 2020, *ApJ*, 897, 100, doi: [10.3847/1538-4357/ab9809](https://doi.org/10.3847/1538-4357/ab9809)
- van Son, L. A. C., de Mink, S. E., Callister, T., et al. 2022, *ApJ*, 931, 17, doi: [10.3847/1538-4357/ac64a3](https://doi.org/10.3847/1538-4357/ac64a3)
- Vink, J. S., de Koter, A., & Lamers, H. J. G. L. M. 2001, *Astronomy and Astrophysics*, 369, 574, doi: [10.1051/0004-6361:20010127](https://doi.org/10.1051/0004-6361:20010127)
- Wang, Y.-H., McKernan, B., Ford, S., et al. 2021, *ApJL*, 923, L23, doi: [10.3847/2041-8213/ac400a](https://doi.org/10.3847/2041-8213/ac400a)
- Webbink, R. F. 1984, *ApJ*, 277, 355, doi: [10.1086/161701](https://doi.org/10.1086/161701)
- Xu, X.-J., & Li, X.-D. 2010, *ApJ*, 716, 114, doi: [10.1088/0004-637X/716/1/114](https://doi.org/10.1088/0004-637X/716/1/114)
- Zevin, M., & Bavera, S. S. 2022, *ApJ*, 933, 86, doi: [10.3847/1538-4357/ac6f5d](https://doi.org/10.3847/1538-4357/ac6f5d)